Acoustically driven optical phenomena in bulk and low-dimensional semiconductors

2001 J. Opt. A: Pure Appl. Opt. 3 S82

(http://iopscience.iop.org/1464-4258/3/4/364)

INSTITUTE OF PHYSICS PUBLISHING JOURNAL OF OPTICS A: PURE AND APPLIED OPTICS
J. Opt. A: Pure Appl. Opt. **3** (2001) S82–S86 www.iop.org/Journals/oa PII: S1464-4258(01)18877-X

Acoustically driven optical phenomena in bulk and low-dimensional semiconductors

I V Ostrovskii[1], O A Korotchenkov[1], O Ya Olikh[1], A A Podolyan[1], R G Chupryna[1] and M Torres-Cisneros[2]

[1] Faculty of Physics, Kiev Taras Shevchenko University, Kiev 01022, Ukraine
[2] Facultad de Ingenieria, Universidad de Guanajuato, Salamanca 36730, Mexico

Received 9 November 2000, in final form 30 April 2001

Abstract
The purpose of this paper is to present new acousto-optical effects in semiconductors. Here we discuss acoustically driven carrier diffusion length and photovoltaic effect in Si and SiGe heterostructures, acoustically driven radiative recombination kinetics in ZnSe/ZnS quantum wells and acousto-photo-reflectance from GaAs epitaxial layers. We argue that acoustic driving can significantly affect the carrier dynamics in bulk and low-dimensional semiconductors.

Keywords: Photovoltaic effect, carrier diffusion length, radiative recombination kinetics, carrier dynamics

1. Introduction

During recent years, a number of new phenomena have emerged in acousto-optical studies. The generation of light by a bounded acoustic beam at the surface of piezoelectric crystals has been classified as a new class of crystal sonoluminescence [1]. Hydrogen redistribution at ultrasonic loading has been shown to strikingly affect photoluminescence in polycrystalline silicon films [2]. Acoustically driven photoconductivity and optical absorption have been observed in a variety of materials [3]. A new contactless electroreflectance method employing acoustic waves has been used to characterize semiconductors [4] and semiconductor heterostructures [5]. An idea running through these studies is the remarkable changes in crystal defect concentrations as well as in electric charges of point defects and dislocations at sufficiently high acoustic driving amplitudes [1,3,6,7]. Several investigations have shown that the complete understanding of acoustically driven optical effects in semiconductors would also involve the analysis of piezoelectric fields accompanying acoustic waves [4, 8].

In this paper, we present new acousto-optical effects observed in bulk silicon, SiGe/Si heterostructures, GaAs epitaxial layers and ZnSe/ZnS quantum wells. We show that acoustic driving can significantly affect dynamics of photoexcited carriers in semiconductors as well as carrier diffusion length, and this can be particularly important for device applications utilizing accumulation of charges and photovoltage effects.

2. Experiments

A number of samples and a variety of experimental techniques are employed in this paper. Acoustically driven photoelectric effects are taken in 340 μm thick solar grade (100) Cz-p-Si wafers doped with boron ($\approx 10^{16}$–10^{17} cm^{-3}). In these experiments, a CVD-grown $Si_{0.83}Ge_{0.17}$/Si heterostructure is also employed. The thicknesses of a SiGe layer and a (100) Si substrate are roughly 1 and 300 μm, respectively.

The diffusion length L of minority carriers in Si is computed by measuring the spectral dependence of the surface photovoltage signal measured with a capacitance technique [9]. The capacitance electrode is formed on the sample surface, which is opposite to that illuminated with light. The photovoltage signal in the SiGe/Si heterostructure is taken between the ohmic contact formed on the bottom Si face and the gold contact deposited on the SiGe layer. The latter is illuminated with a pulse light and the decay of the photovoltage signal is obtained. All these measurements are performed at room temperature.

Acoustically driven dynamics of photoexcited carriers are furthermore studied in ZnSe/ZnS heterostructures when three-, five-and seven-monolayer thick ZnSe is sandwiched between ZnS cap and barrier layers grown on a GaAs(001) substrate (see figure 1). In these measurements, the photoluminescence is excited by picosecond pulses of 4.0 eV light of a Rhodamine 6G dye laser pumped by a mode-locked YAG laser, and the temporal evolution of the emission intensity is taken at liquid helium temperature by a Hamamatsu streak camera.

Acoustically driven changes in optical reflectivity are taken with a Te-doped GaAs epitaxial layer (free carrier con-

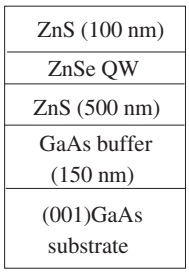

Figure 1. A sketch of the ZnSe/ZnS structure.

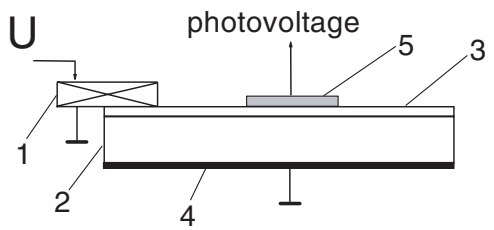

Figure 2. Experimental set-up used to excite plate vibrations: 1, piezoceramic transducer; 2, substrate; 3, thin layer; 4, ohmic contact; 5, semitransparent metallic layer.

centration is 6×10^{15} cm^{-3}) MBE grown on a GaAs(100) substrate (1.4×10^{18} cm^{-3}). The thicknesses of the layer and the substrate are 1.45 and 350 μm, respectively. The sample is illuminated with tungsten lamp light dispersed by a monochromator in the near-normal incidence geometry whereas the reflected light is collected on a photoelectric detector. The slits of the monochromator are set sufficiently narrow to resolve fully all the spectral features that are reported below. The spectra of the reflected light with intensity I_R are registered in the energy range close to the bandgap of GaAs and the reflectivity $R = I_R/I_0$ with I_0 the intensity of the incident light is then computed. Both the initial spectrum of R_0 without ultrasound and that of R_{US} under ultrasonic (US) loading are measured, and the differential spectra are obtained from these two according to

$$\frac{\Delta R}{R_0} = \frac{R_{US} - R_0}{R_0}.$$

The samples are typically plate shaped with a thickness range from 300 μm to 1 mm and linear dimensions $\approx 3 \times 15$ mm^2. Acoustic vibrations are excited in the frequency range from 0.2 to 5.5 MHz by mounting a piezoceramic transducer 1 on the sample surface 3 as shown in figure 2. An rf voltage U supplied from a generator drives the transducer, resulting in acoustic oscillations of the samples. The voltage amplitude is continuously adjustable between $U = 0$ and $\approx$40 V, and the corresponding strain amplitude inside the sample is estimated from a quality factor of the vibrating system.

Some measurements are performed by mounting a sample on a $LiNbO_3$ delay line, which drives the surface acoustic waves. In this set-up, the sample–piezoelectric substrate arrangement is acoustically mismatched, so electric fields penetrate into the sample, thus determining the observed driving effect. The amplitude of the electric potential φ_0 can be approximated by [10]

$$\varphi_0^2 = \frac{2K^2 P}{\Omega w \varepsilon_0 (1+\varepsilon)},$$

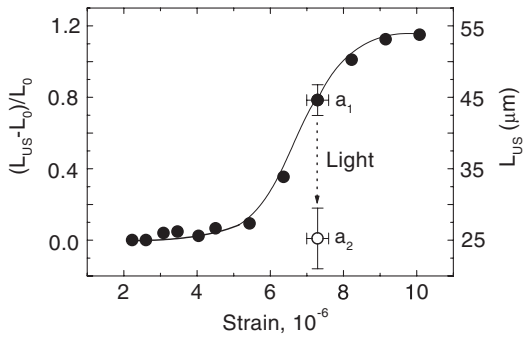

Figure 3. Dependence of the diffusion length of minority carriers versus acoustic strain amplitude taken from a Cz-p-Si wafer. L_0 indicates the diffusion length in the absence of acoustic driving while L_{us} corresponds to that measured at US loading. The value of L_0 is 15–25 μm for different samples. The US frequency is 780 kHz. Points a_1 and a_2 display the data taken in darkness and under light illumination, respectively.

where K^2 is the electromechanical coupling constant, ε_0 and ε are the dielectric constants of free space and $LiNbO_3$, respectively, w is the acoustic beam width, Ω is the frequency of the surface acoustic wave and $P \propto U^2$ is the acoustic power estimated from the radiation conductance of an interdigital transducer generating the wave. Then the electric field amplitude is simply $F_{US} = k\varphi_0 = (\Omega/V)\varphi_0$ with k the wavenumber and V the velocity of the surface acoustic wave.

3. Acoustically driven diffusion length and photovoltaic effect in Si and SiGe heterostructures

The photogenerated carriers diffuse away from the illuminated region and sample photoelectricity is often dominated by carrier diffusion and capture processes. Therefore, we attempt to acoustically drive the diffusion length of minority charge carriers in Cz-p-Si wafers. The results shown in figure 3 exhibit the striking effect of ultrasonic loading on the diffusion length L. It is seen that a length increase as high as a factor of two is observed. The acoustostimulated change in L is reversible, and the value of L relaxes only gradually with time after US is off. Typically, the initial value L_0 has been achieved in $\sim 10^2$ min. It should be stressed that the ultrasonic effect on the diffusion length L_{us} strongly depends on acoustic strain amplitude ε and exhibits threshold behaviour. As seen in figure 3, the threshold US strain is $\varepsilon \sim 4 \times 10^{-6}$ which corresponds to acoustic intensity $W_{us} \sim 0.5$ W cm^{-2}. It is also seen in figure 3 that the saturation of the dependence $L_{us}(\varepsilon)$ is observed above $\varepsilon \sim 8 \times 10^{-6}$ ($W_{US} \sim 2.5$ W cm^{-2}).

It is not the intention of this paper to give a detailed microscopic picture of the observed effect. We can only speculate on the trends that might account for the presented results. Thus, the minority carrier diffusion length is believed to depend rather sensitively on the carrier recombination at deep traps and this is particularly true at room temperatures [11, 12]. The traps could arise both from point defects, intrinsic and impurity ones, and extended defects such as dislocations which can interact with each other. It has been found that in Cz-Si the diffusion length L is often controlled by heavy metal impurities. For example, doping with Fe impurities is a very effective means to decrease L

because the electron capture probability is rather high for Fe-ion-related centres [12]. Furthermore, the ions of $Fe^{+,2+}$ in boron-doped p-Si (in excess of 10^{15} cm^{-3}) tend to form Fe_i–B_{Si} pairs at room temperature [13, 14] with interstitial Fe and B in a silicon site. The electron capture probability of these centres is remarkably smaller than that of a single Fe ion. As the US loading can destroy the Fe_i–B_{Si} pairs, this would lead to decreased lengths L_{us} in acoustically treated samples, and this effect has previously been given particular consideration [15, 16]. Increased L_{us} has also been attained in ultrasonically treated polycrystalline silicon [15], although the conclusive explanation of this fact is still lacking. It has been suggested that enhanced gettering of point defects in the treated sample would probably account for the length enhancement [15] and this may indeed be the case in the samples with extended grain boundaries.

To our knowledge, at present, no diffusion length enhancement in bulk silicon has been reported as a dynamical effect under ultrasonic action. One should obviously search for the mechanism which is capable of explaining the results presented in figure 3. We believe that the existence of two types of Fe_i–B_{Si} pairs corresponding to two nearest neighbours in the [111] and [100] directions [13] should be taken into account. As the second site (B type) for the pair lies higher in energy than the first site (A type), it is initially much less populated than the type A site. Acoustic driving probably enhances the population of the second site compared with the first site when the ion overcomes the migration barrier, which is typically of the order of 0.1 eV. Furthermore, acoustic driving probably enhances the concentration of Fe ions capturing one electron (for example, Fe^+ versus Fe^{2+}). It is essential to note that the energy gap between Fe^{2+} and Fe^+ is implied to be substantially smaller in the [100] direction (B type) [13, 17]. Therefore, we arrive at the final state of the recharged Fe atom pairing in the type B site with reduced electron capture probability.

There has been found direct experimental evidence that supports the presented mechanism. Thus, illuminating a sample with white light at room temperature is known to destroy Fe–B pairs with a subsequent decrease in the diffusion length due to increased concentration of liberated Fe [15]. In our experiments, the sample illumination also leads to decreased L (∼15% in the absence of the driving). When ultrasonic loading is applied and enhanced L is attained, the light illumination has been found to strikingly decrease the diffusion length such that the ultrasonic effect on L may be completely quenched. This result is illustrated in figure 3 by point a_2 taken under light illumination. It is seen that, measured at constant ultrasonic strain, the L value decreases from point a_1 to point a_2 on illuminating the sample. Therefore, the featuring of the Fe–B pairs in the presented effect is implied.

The driving effect is further studied in optically excited samples. For this purpose, SiGe/Si and ZnSe/ZnS heterostructures are employed. In the $Si_{0.83}Ge_{0.17}$/Si sample, acoustic loading tends to remarkably modify the photovoltage temporal evolution. For example, the dynamics of photoexcited carriers after the light is off exhibits rather complicated behaviour (see figure 4, curve 1). The rapid decrease in photovoltage seen just after the light is off is probably dominated by the band-to-band recombination

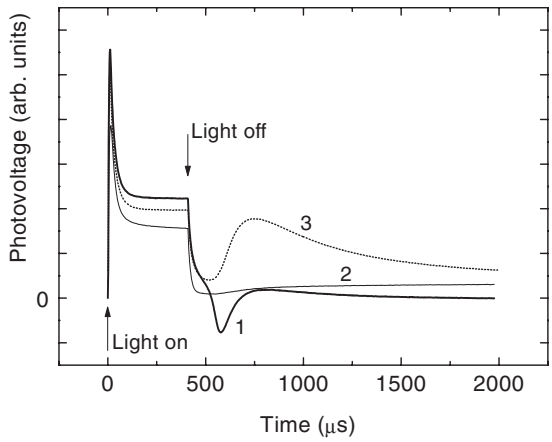

Figure 4. Temporal evolution of photovoltage in $Si_{0.83}Ge_{0.17}$/Si heterostructure after the light is turned on and off: (1) before US loading, (2) at loading with $\varepsilon \sim 2 \times 10^{-6}$ and (3) 16 h after US loading. The illumination is achieved with a 835 nm LED. The US frequency is 3.1 MHz.

whereas the following increase in the signal is indicative of a defect recharge. Application of acoustic driving at sufficiently high strain amplitude, above $\varepsilon \sim (2\text{–}6) \times 10^{-6}$, dramatically affects the long-time kinetics (curve 2 in figure 4). This effect may be due to a threshold redistribution of interface defects that alters the filling of local states determining the long-time relaxation of photovoltage. The defect migration in an ultrasonic field is probably achieved so that the initial signal cannot be restored even within some hours (curve 3 in figure 4).

4. Acoustically driven radiative recombination kinetics in quantum wells

In low-dimensional heterostructures, the distances involved are typically less than 1000 Å, implying diffusion times of the order of 100 ps or even less. As the capture of photoexcited carriers into quantum wells is very rapid, of the order of 1 ps, their diffusion within the well and their capture to interface bound states often dominate the radiative recombination. Acoustic driving of the rise time of the photoluminescence of localized excitons in a ZnSe/ZnS quantum well system is shown in figure 5. It is seen that the driving can affect the recombination kinetics substantially, particularly above some threshold value (i.e. above $F_{US} \approx 2.5\,kV\,cm^{-1}$ in figure 4). We thus conclude that the capture coefficient for the trap decreases in acoustically driven electric fields that can be treated as enhanced diffusion of the photoexcited carriers within the well.

5. Acousto-photo-reflectance from GaAs epitaxial layers

The optical properties of semiconductors depend on the coupling of their various oscillators to the radiation field. The oscillators may particularly include excitons, phonons or lattice defects. As acoustic driving causes the defect recharge, this would disturb the dielectric function or the refractive index, which can be monitored by analysing acoustically driven spectra of a sample reflection. The problem can now be

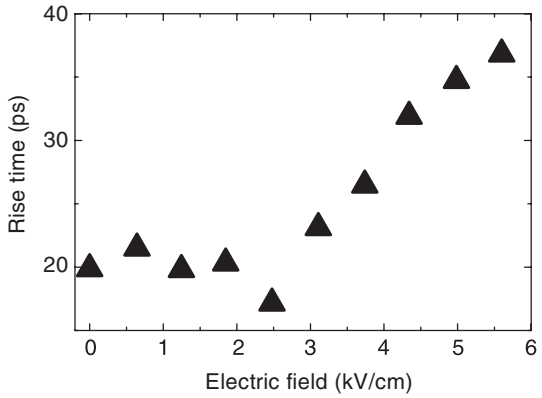

Figure 5. Bound exciton emission rise time in the ZnSe/ZnS heterostructure versus driving piezoelectric field. The US frequency is 10 MHz.

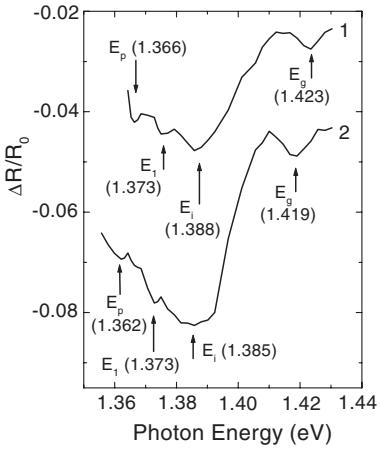

Figure 6. Spectral dependence of the relative change in the light reflectivity in GaAs:Te/GaAs caused by acoustic driving at $U = 18$ V (1) and 24 V (2). The US frequency is 258 kHz.

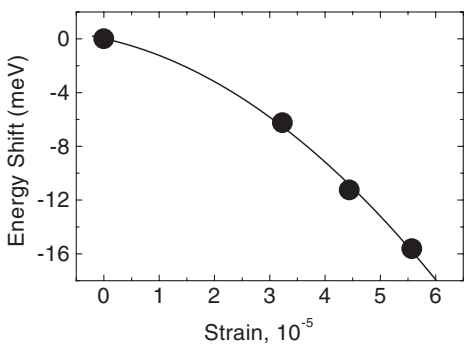

Figure 7. The energy shift of the light reflectivity in GaAs:Te/GaAs taken at about E_g with increasing driving strain amplitude.

discussed in the framework of a simplified harmonic oscillator model, so we may write the complex dielectric function

$$\varepsilon = 1 + \frac{fNe^2/m}{\omega_0^2 - \omega^2 - i\omega\Gamma},$$

where f is the oscillator strength, N is the number of oscillators per unit volume (occupation of defect energy levels), e and m are the electron charge and effective mass, respectively, ω_0 can be interpreted as the electron transition frequency or optical phonon energy, ω is the frequency of the optical field and Γ is the Lorentzian broadening parameter. Taking $\Gamma \to 0$ we find the relative change in the light reflectivity

$$\frac{\Delta R}{R} \propto \frac{fNe^2}{m}\left[-\frac{2\omega_0\Delta\omega_0}{(\omega_0^2-\omega^2)^2} + \frac{\Delta N}{N}\frac{1}{\omega_0^2-\omega^2}\right].$$

It is seen that the acoustically induced reflectivity change is a sum of two terms. The first term is proportional to $\Delta\omega_0$ and corresponds to changes in the binding energy of the electron (or hole) at the trapping centre at acoustic driving. The second term may arise from the change in the energy level occupation due to the defect recharge. Therefore, the driving-induced changes in the electron occupation of defect states would remarkably enhance $|\Delta R/R|$ at the optical frequency $\omega \to \omega_0$. A peak in the reflectivity is also expected in the spectral range close to the bandgap energy, which is due to an acoustically driven change in the energy gap E_g. The bandgap change turns out to be due to the stress, thermal heating and piezoelectric field accompanying ultrasonic loading.

This is exactly what is seen in figure 6, illustrating acoustically driven changes in R. Shown by arrows E_1 are the lines at about 1.37 eV, which can arise from the electronic transitions with arsenic vacancies, whereas the lines at about 1.42 eV indicated by arrows E_g are due to the transitions between the valence and conduction bands. Both the lines have previously been discussed in the literature [5]. To mediate between the suggested assignment of the lines E_1 and E_g displayed in figure 6 and the likely influence of the heating effect on the line appearance, shown in figure 7 is the low-energy shift of the sample reflectivity, which is taken at about the bandgap energy with increasing driving amplitude. It is seen that the observed shift does not exceed 16 meV for the maximum strain amplitude. In contrast, on the assumption that the wide band between 1.36 and 1.40 eV seen in figure 6 originates from the thermally reduced bandgap, the maximum shift in figure 7 is expected to be substantially greater, about 40 meV. Therefore, consistent with the interpretation of the E_g line as the band-to-band electronic transitions, it undergoes $\approx$10 meV red shift in figure 6, demonstrating the reduction in the bandgap.

In the spectra of figure 6, there appear two lines peaked at about 1.39 eV (marked by E_i) and 1.36 eV (E_p). The lines exhibit a red shift with increasing driving strain amplitude although, with respect to the bandgap energy, the computed energy positions of the lines ($E_g - E_{i,p}$) are found to be nearly independent of ε and yield 34 and 57 meV, respectively. A complete characterization of these lines requires the analysis of data from a variety of techniques. Here, we attempt only to gain tentative insight into the origin of the observed lines. Thus, the energy depth of about 31 meV inside the bandgap of GaAs has been attributed to a Zn impurity in a gallium site [18]. Consequently, we might suggest that the E_i line probably arises from the impurity levels. Then, since the coupling of the LO phonons to the conduction electrons is strong, one could expect the appearance of appropriate lines in the acoustically driven spectra presented in figure 6. Their observation is reliant upon the fact that the probability of the electron–phonon interaction is realized as a process involving

two phonons due to the momentum conservation law. Taking the (LO + LO) phonon energy of 59 meV [19] yields the conclusion that the correspondence between the observed line marked E_p in figure 6 (57 meV with respect to the bandgap energy) and the (LO + LO) phonon energy is good. Therefore, the phonon origin of the E_p line is assumed.

6. Conclusion

A number of new acousto-optical effects in semiconductors are reported. It is shown that the diffusion length of minority charge carriers in silicon can be remarkably enhanced at acoustic loading. It is argued that the length increase may tentatively be explained by the reorientation and the recharge of the Fe–B pairs in acoustic fields. It is further shown that acoustic loading can significantly affect the temporal evolution of the photoexcited carriers in SiGe/Si and ZnSe/ZnS heterostructures, which is likely to be due to acoustically driven redistribution of defects and defect recharge processes. Finally, it is found that acoustic driving can effectively modify the light reflectivity from GaAs epitaxial layers, such that the defect-related energy levels and the optical phonon energies can be deduced from the reflectivity spectra affected by ultrasound.

References

[1] Ostrovskii I V and Das P 1997 Observation of a new class of crystal sonoluminescence at piezoelectric crystal surface *Appl. Phys. Lett.* **70** 167–9

[2] Koshka J, Ostapenko S, Ruf T and Zhang J M 1996 Activation of luminescence in polycrystalline silicon thin films by ultrasound treatment *Appl. Phys. Lett.* **69** 2537–9

[3] Ostrovskii I V and Korotchenkov O A 1992 Characterization of unstable point defects in crystals *Solid State Commun.* **82** 267–70

[4] Fritz I J and Brennan T M 1997 Semiconductor characterization by a new contactless electroreflectance technique employing surface acoustic waves *Semicond. Sci. Technol.* **12** 19–21

[5] Ostrovskii I V, Korotchenkov O A, Burbelo R M and Walther H G 2000 Characterization of semiconductor heterostructures by acousto-optical perturbation technique *Mater. Sci. Eng.* B **76** 139–44

[6] Olikh Ya M and Shavlyuk Yu I 1996 Acoustostimulated reduction of $1/f$ noise in subblock crystals of $Cd_{0.2}Hg_{0.8}Te$ *Solid State Phys.* **38** 3365–71

[7] Ostrovskii I V, Korotchenkov O A, Goto T and Grimmeiss H G 1999 Sonoluminescence and acoustically driven optical phenomena in solids and solid–gas interfaces *Phys. Rep.* **311** 1–46

[8] Streibl M, Wixforth A and Gossard A C 1999 Imaging of acoustic charge transport in semiconductor heterostructures by surface acoustic waves *Appl. Phys. Lett.* **75** 4139–41

[9] Lagowski J, Edelman P, Dexter M and Henley W 1992 Non-contact mapping of heavy metal contamination for silicon IC fabrication *Semicond. Sci. Technol.* A **7** 185–92

[10] Lakin M 1971 Perturbation theory for electromagnetic coupling to elastic surface waves on piezoelectric substrates *J. Appl. Phys.* **42** 899–906

[11] Schroder D K 1997 Carrier lifetimes in silicon *IEEE Trans. Electron. Devices* **44** 160–70

[12] Hanglaiter A 1987 Nonradiative recombination via deep impurity levels in silicon: experiment *Phys. Rev.* B **35** 9149–61

[13] Nakashima H, Sadoh T and Tsurushima T 1994 Electrical and thermal properties of structurally metastable iron–boron pairs in silicon *Phys. Rev.* B **49** 16 983–93
Assali L V C and Leite J R 1987 Electronic properties of the iron–boron impurity pair in silicon *Phys. Rev.* B **36** 1296–9

[14] Zoth G and Berholz W 1990 A fast, preparation-free method to detect iron in silicon *J. Appl. Phys.* **67** 6764–71

[15] Ostapenko S S, Jastrzebski L, Lagowski J and Sopori B 1994 Increasing short minority carrier diffusion lengths in solar-grade polycrystalline silicon by ultrasound treatment *Appl. Phys. Lett.* **65** 1555–7
Ostapenko S S, Jastrzebski L and Sopori B 1995 Change of minority carrier diffusion length in polycrystalline silicon by ultrasound treatment *Semicond. Sci. Technol.* **10** 1494–500

[16] Ostapenko S S and Bell R E 1995 Ultrasound stimulated dissociation of Fe–B pairs in silicon *J. Appl. Phys.* **77** 5458–60

[17] Overhof H and Weihrich H 1997 *Ab initio* total-energy calculations for iron-acceptor pairs in silicon *Phys. Rev.* B **55** 10508–14

[18] Neu G, Teisseire M, Freundlich A, Horton C and Ignatiev A 1999 Donor–acceptor-pair spectroscopy of GaAs grown in space ultravacuum *Appl. Phys. Lett.* **47** 3341–3

[19] Pankove J I 1975 *Optical Processes in Semiconductors* (New York: Dover)